Structural Analysis of Thrombin Complexed with Potent Inhibitors Incorporating a Phenyl Group as a Peptide Mimetic and Aminopyridines as Guanidine Substitutes

Roger Bone,* Tianbao Lu, Carl R. Illig, Richard M. Soll, and John C. Spurlino

3-Dimensional Pharmaceuticals Inc., Eagleview Corporate Center, 665 Stockton Drive, Suite 104, Exton, Pennsylvania 19341

Received November 21, 1997

The structure of the noncovalent complex of human α-thrombin with a nonpeptide inhibitor containing a central phenyl scaffold, *N*-[2-[5-methyl-3-(2-chlorophenylsulfonyloxy)phenoxy]-ethyl]-*N*-methyl-4-aminopyridine (**1**), has been determined to 2.20 Å resolution. In addition, the thrombin-bound structures of two distinct amino acid-based inhibitors (**3** and **4**) containing different aminopyridine-derived guanidine mimetics have been determined. Each compound occupies the same region of the active site and projects an aminopyridine, a central hydrophobic group, and an aryl group, into the S_1, S_2, and aryl subsites on thrombin. Nonpeptide **1** forms only one direct intermolecular hydrogen bond to the thrombin active site and forms no hydrogen bonds to ordered molecules of solvent. Close contacts are observed between main-chain carbonyl groups on thrombin and the edges of the central phenyl and aminopyridine rings and the sulfonyl group of **1** such that atoms carrying opposite partial charges are juxtaposed. Aminopyridine groups in **3** and **4** also form close contacts with the edges of carbonyl groups on thrombin and are flexibly accommodated in the S_1 subsite. Superposition of the bound conformations of **1** and D-Phe-Pro-amidobutylguanidine (**2**) revealed that the central phenyl scaffold of **1** substitutes for the peptide main chain of **2**.

Among the greatest challenges in modern drug discovery is the conversion of peptide lead molecules with intermediate potency into high potency, nonpeptide compounds with pharmacological properties that are appropriate for use as drugs. Recent efforts have led to the discovery of peptide residue replacements that have many of the characteristics desirable in a drug: low molecular weight, rigidity, limited hydrophilicity, and no chiral centers. For example, antagonists of the IIb/IIIa receptor have been identified in which the central glycine of Arg-Gly-Asp-Trp (**9**) is replaced with the phenolic ring of a tyrosine[1,2] (**8**; see Figure 1). In another example, inhibitors of the Ras farnesyl transferase have been discovered in which the three C-terminal residues of the natural Cys-Val-Ile-Met ligand (**7**) are replaced with a substituted biphenyl system[3,4] (**6**). Finally, thrombin inhibitors have been developed recently in which the central Pro residue of D-Phe-Pro-descarboxy-Arg[5] (**2**) can be replaced with a phenyl ring[6,7] in *N*-[2-[5-methyl-3-(2-chlorophenylsulfonyloxy)phenoxy]-ethyl]-*N*-methyl-4-aminopyridine (**1**).

In each of these examples an entire amino acid residue is replaced with a phenyl group with greater rigidity and more limited hydrogen-bonding capabilities. In each case, potency with the phenyl group replacement is improved by 1 order of magnitude over that of the peptide ligand (Table 1) and a number of questions arise. Do these phenyl groups occupy the same position in the binding site as the peptide residues which they replace? How can phenyl groups with limited hydrogen-bonding capacity substitute for extremely polar peptide bonds? Why are the potencies of these nonpeptides superior to the peptide leads which they replace? Understanding the structural basis for the inhibition of thrombin by compounds such as **1** is also of interest because of the use of an aminopyridine group as a substitute for a guanidine function.

In this work we report the determination of the structure of the intermolecular complex of **1** with thrombin using X-ray crystallography and provide a detailed description of the structural basis for the ability of a phenyl group to substitute for a peptide residue. For comparison, we have independently determined the structure of the thrombin complex with a noncovalent peptide inhibitor[5] (**2**). Although more elaborate and potent analogues of **2** have been discovered,[8−10] **2** is an ideal comparator to **1** because they have similar size, surface area, and complexity and **2** retains peptide character similar to substrates. Our results show that although **1** forms only a single, direct hydrogen bond with the enzyme, it occupies the same location in the active site as peptide inhibitor **2** which forms six direct hydrogen bonds and two water-mediated hydrogen bonds with thrombin. In addition, we have determined the structures of thrombin complexes with three classes of inhibitor, each containing a different aminopyridine-based guanidine mimetic. The aminopyridine groups in compounds **1**, **3**, and **4** appear to interact with the S_1 pocket[11] in novel ways and each compound presents the pyridine group to the binding pocket in a different manner.

Experimental Procedures

Human α-thrombin was purchased from Enzyme Research Laboratories and crystallized at 4 °C in a complex with sulfated hirudin 53−65 (Bachem Biosciences) as previously described.[12,13] Complexes of thrombin with the hirudin fragment and active site-directed inhibitors were formed by adding inhibitor solutions to standing vapor diffusion drops (2 μL)

S0022-2623(97)00796-6 CCC: $15.00
Published on Web 05/15/1998

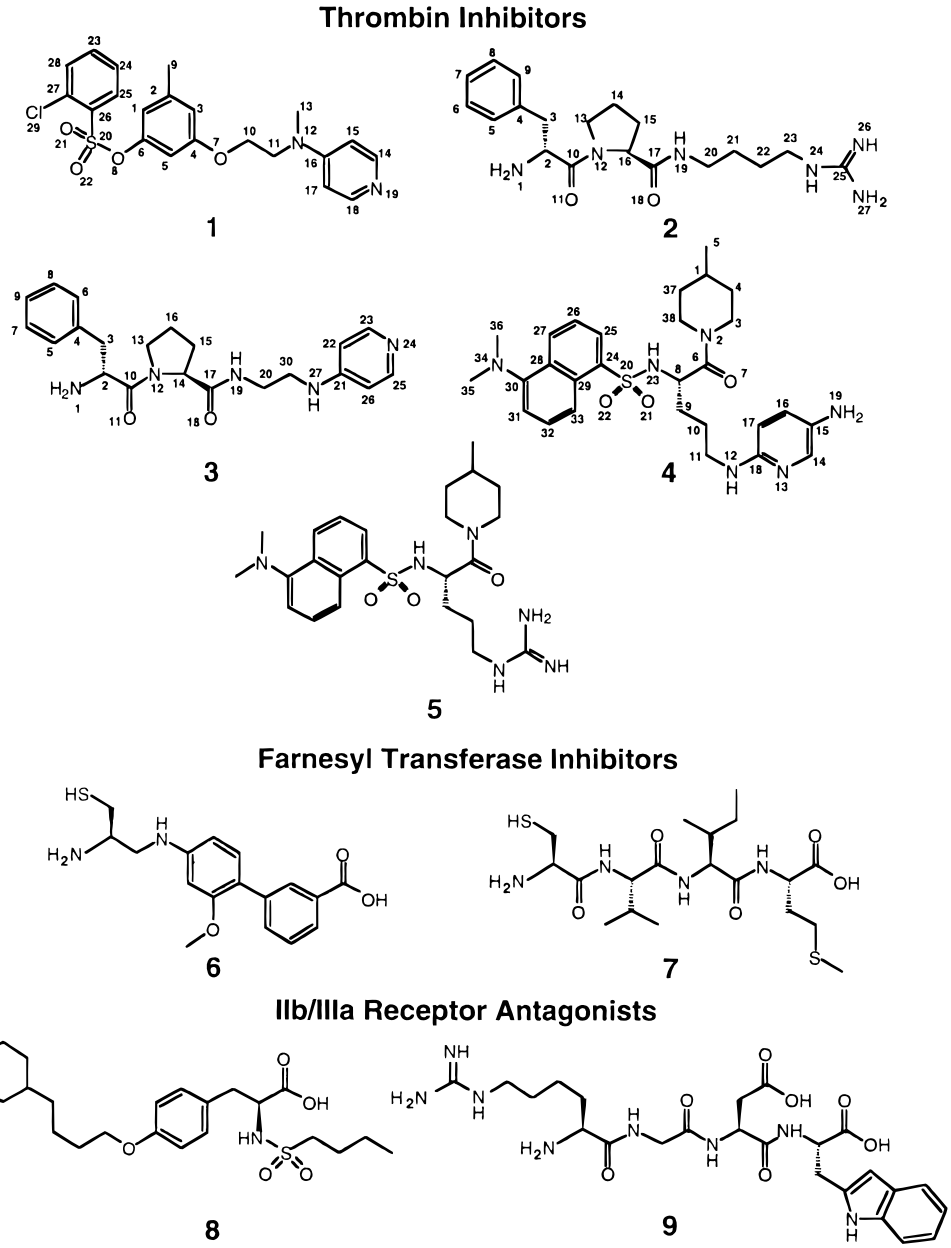

Figure 1. Structures of nonpeptide and corresponding peptide inhibitors of thrombin, farnesyl transferase, and antagonists of the IIb/IIIa receptor.

Table 1. Potency of Peptide Leads and Phenyl Group Amino Acid Surrogates

compd	target	potency (nM)	ref
1	thrombin	24[a]	6
2	thrombin	180[a]	5
3	thrombin	4100[a]	15
4	thrombin	360[a]	15
5	thrombin	300[b]	49
6	farnesyl transferase	40[b]	3
7	farnesyl transferase	200[b]	3
8	IIb/IIIa receptor	9[b]	2
9	IIb/IIIa receptor	1700[b]	2

[a] K_i. [b] IC_{50}.

containing large single crystals of α-thrombin. Crystals were undamaged by this procedure and were mounted for data collection 4−5 h after the addition of inhibitors. Compounds **1**−**4** were synthesized using published procedures.[6,14,15] The HCl salt of **1** was dissolved in DMSO at a concentration of 200 mM and then diluted to 4 mM in 28% PEG 8000 containing 100 mM phosphate buffer (pH 7.3), 0.15 M NaCl, and 3 mM NaN_3. An aliquot (1 μL) of this solution was added to a drop (2 μL) containing single thrombin crystals to produce a final inhibitor concentration of 1.3 mM. Inhibitor **2** was dissolved in 25% PEG 8000 containing 100 mM phosphate buffer, 0.2 M NaCl, and 3 mM NaN_3 at a final concentration of 4.2 mM. An aliquot (0.5 μL) of this solution was added to a drop (2 μL) containing a single thrombin crystal to yield a final inhibitor concentration of 0.8 mM. Inhibitor **3** was dissolved in DMSO containing 0.98 equivalents of HCl at a concentration of 200 mM. This solution was diluted into 28% PEG 8000 containing 100 mM phosphate buffer, 0.15 M NaCl, and 3 mM NaN_3 to produce a final concentration of 6 mM. An aliquot (1.0 μL) of this solution was added to a drop (2 μL) containing a single thrombin crystal to yield a final inhibitor concentration of 2.0 mM. Inhibitor **4** was dissolved in DMSO (100 mM) then diluted into buffer to produce a solution of 25% PEG 8000 and 4% DMSO containing mM phosphate buffer, 0.2 M NaCl, and 3 mM NaN_3 with **4** at a final concentration of 1.0 mM. An aliquot (2.0 μL) of this solution was added to a drop (2 μL) containing a single thrombin crystal to yield a final inhibitor concentration of 0.5 mM.

Data for each ternary complex were collected from a single crystal using monochromatic Cu Kα X-rays ($\lambda = 1.5418$ Å) from

Table 2. Statistics for Structure Determinations of Human α-Thrombin Complexes with Sulfated Hirudin 53−65 and Inhibitors

	ternary complex			
parameter	1	2	3	4
space group	C2	C2	C2	C2
cell dimensions	$a = 70.5$ Å	$a = 70.2$ Å	$a = 70.9$ Å	$a = 71.4$ Å
	$b = 71.8$ Å	$b = 71.8$ Å	$b = 71.8$ Å	$b = 72.7$ Å
	$c = 72.3$ Å	$c = 72.2$ Å	$c = 72.7$ Å	$c = 72.6$ Å
	$\beta = 100.52°$	$\beta = 100.85°$	$\beta = 100.52°$	$\beta = 100.44°$
resolution	8.0−2.20 Å	8.0−2.25 Å	8.0−1.8 Å	8.0−2.35 Å
R_{merge}[a]	0.073	0.071	0.083	0.101
% $I/\sigma_I > 2$	85.3%	87.4%	86.6%	83.6%
av. I/σ_I	12.9, 3.6	16.5, 5.3	12.3, 3.5	10.7, 3.5
completeness	87.7%	88.0%	88.1%	83.6%
refinement				
R_{cryst}[b]	0.18	0.18	0.19	0.19
rms bond dev	0.011 Å	0.011 Å	0.010 Å	0.013 Å
rms angle dev	1.3°	1.3°	1.2°	1.5°
B-factors				
protein				
average B	24.5 Å^2	26.6 Å^2	21.1 Å^2	23.9 Å^2
active site B	19.4 Å^2	21.2 Å^2	16.6 Å^2	17.7 Å^2
rms bonded (MC)	2.4 Å^2	2.5 Å^2	2.4 Å^2	2.4 Å^2
rms bonded (SC)	3.9 Å^2	4.1 Å^2	3.9 Å^2	3.8 Å^2
inhibitor				
min	18.6 Å^2	18.6 Å^2	19.2 Å^2	24.9 Å^2
max	37.6 Å^2	29.3 Å^2	39.2 Å^2	16.7 Å^2
average	27.3 Å^2	22.1 Å^2	26.1 Å^2	33.6 Å^2

[a] $R_{merge} = (\Sigma\Sigma|I_j(h) - \langle I(h)\rangle|/(\Sigma\Sigma I_j(h))$; summations done over all reflections from a crystal. [b] $R_{cryst} = (\Sigma|F_{obs} - F_{calc}|)/(\Sigma|F_{obs}|)$.

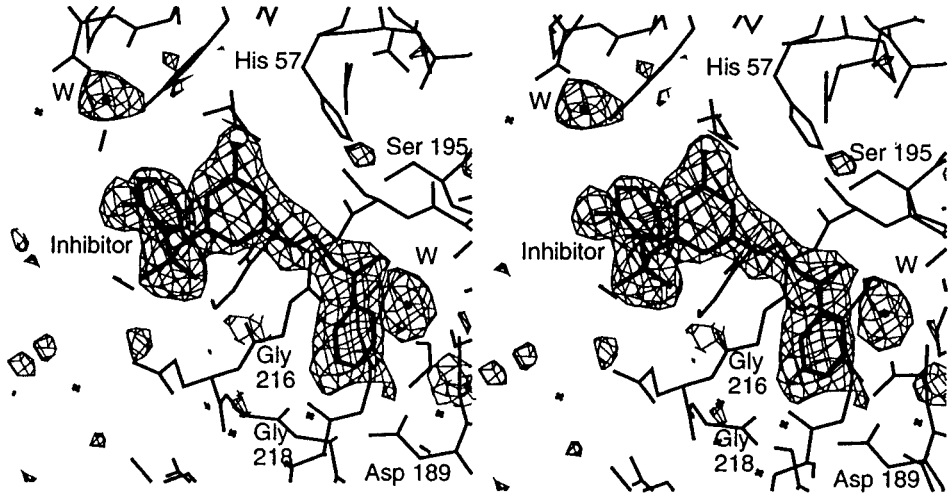

Figure 2. Stereodrawing of a difference electron density map ($|F_o| - |F_c|$) of the thrombin complex with **1**. Structure factors and phases were calculated as described in the text.

an Enraf Nonius generator and a Rigaku automated X-ray imaging system. Cell dimensions and data reduction statistics for each of the inhibitor complexes are shown in Table 2. Data to 2.0 Å resolution were also collected for the thrombin complex with sulfated hirudin 53−65 and the structure refined to a crystallographic R factor of 0.192 using XPLOR.[16] This structure, minus several active-site water molecules, was used as the starting model for determining the structures of complexes with active site-directed inhibitors. Preliminary positional and temperature factor refinement with inhibitor and solvent deleted was performed using XPLOR,[16] and then difference electron density maps were calculated (Figure 2). The program CHAIN[17] was used to model inhibitors and ordered solvent molecules in difference electron density and for additional adjustment of enzyme and inhibitor atomic positions. The structures were further refined using XPLOR[16] (see Table 1 for refinement statistics). Residues that appeared to be disordered were either left out of the model (A chain residues 1−7 and 30−35 and B chain residues 180−189 and 244) or assigned an occupancy value of 0.0 (disordered side chains). Inhibitor occupancy values were set to unity and not refined. Calculations of molecular surface areas were done using the molecular surfacing algorithm MS.[18,19] The coordinates have been deposited in the Protein Data Bank[20] (BNL 21349, 21376, 21377, 21378).

Results

Thrombin Inhibitor Complexes. Initial difference electron density maps, calculated from atomic coordinates after positional and temperature factor refinement without the inhibitor, clearly revealed the positions of each inhibitor as well as additional solvent molecules which were not included in the difference Fourier calculation (Figure 2). Remarkably, the inhibitors occupy the same binding locations within the active site (Figures 3 and 4). Each inhibitor can be thought of as being composed of three components: a basic P_1 substituent, a central group which acts as a scaffold and/or S_2 binding fragment, and an aryl substituent. Compounds **2** and **3** are based on a proline scaffold, compound **1** on a phenyl scaffold, and compound **4** on an ornithine scaffold. Aminopyridine, phenyl, and chlorophenyl rings in **1** are roughly equivalent to agmatine, Pro and D-Phe

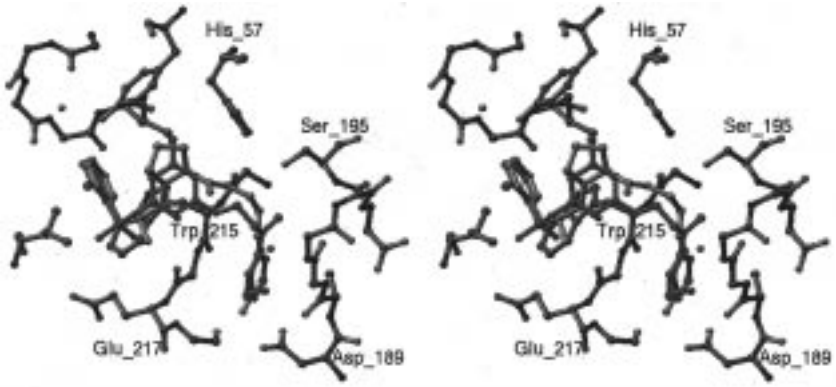

Figure 3. Stereodrawing of the structure of the thrombin-bound conformation of **2** (orange) superimposed on the structure of the thrombin complex with **1** (green). The structures were superimposed using all Cα atoms in thrombin in each structure.

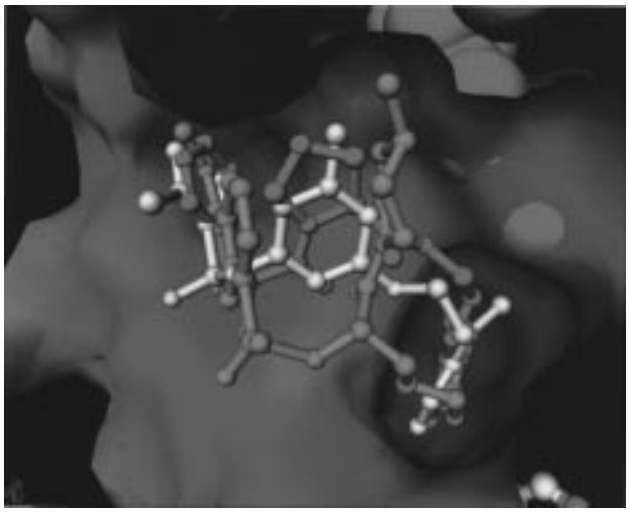

Figure 4. Stereodrawing of the structure of the thrombin-bound conformations of **3** (red) and **4** (blue) superimposed on the structure of the thrombin complex with **1** (white). The structures were superimposed using all Cα atoms in thrombin in each structure.

groups in **2** and aminopyridine, Pro and D-Phe groups, respectively, in **3**. Aminopyridine, methylpiperidine, and dansyl groups in **4** occupy the same binding subsites as the aminopyridine, phenyl, and chlorophenyl rings in **1**. Aryl and basic substituents in each compound are bound by the distal aryl and P_1 pockets of thrombin in similar orientations and positions. However, each inhibitor appears to have a core region or scaffold which interacts with the thrombin active site differently while projecting substituents into these binding subsites (Figures 3 and 4). Thrombin does not appear to adjust significantly in order to accommodate these inhibitors, but slight adjustments (0.1−0.2 Å) relative to the structure of the enzyme in the absence of inhibitor are observed about Asp 189 in the S_1 pocket, Ser 195 and Trp 60D above the S_2 pocket, and Ile 174 in the aryl binding region.

Interaction of Thrombin with Scaffolds. The central phenyl group of **1** roughly occupies the S_2 pocket, lined by residues His 57, Tyr 60A, Trp 60D, Leu 99, and Trp 215, where it is nearly completely removed from solvent. The inhibitor adopts a conformation in which the sulfate sulfur is rotated almost 90° out of the plane of the central orcinol ring (Table 3). Examination of the known single-crystal structures of several arylsulfonate esters reveals the same nearly 90° torsional rotation about the C−O bond of the aryl ester.[21−25] The chlorophenyl ring assumes a conformation in which the 2-chloro substituent is exactly staggered between two sulfonate oxygens with the third sulfonate oxygen in the plane of the ring. On the other side of the phenyl scaffold, the ether is rotated out of the plane of the central ring by nearly 45°. The methylene carbons linking the central phenyl and aminopyridine rings adopt staggered conformations with the carbon proximal to the aminopyridine in the plane of the pyridine ring.

Table 3. Torsional Angles for the Bound Conformation of 1

bond torsion	angle, deg	bond torsion	angle, deg
C5−C4−O7−C10	47	C11−N12−C16−C17	−3
C4−O7−C10−C11	155	C1−C6−O8−S20	98
O7−C10−C11−N12	63	C6−O8−S20−C26	−64
C10−C11−N12−C16	−122	O8−S20−C26−C27	−53

The core region of **1** does not form any direct hydrogen-bonding interactions with thrombin, and only the aryl ether oxygen (O8) is close to a hydrogen-bond donor on thrombin (Gly 216 NH, 3.57 Å). The edge of the central aromatic ring of **1** is in close proximity to the carbonyl group of residue 216 (Figure 3), which is typically involved in key hydrogen-bonding interactions with peptide-based inhibitors (Figure 3). Ordered solvent molecules are not observed near the carbonyl group of Gly 216, though it cannot be ruled out that the carbonyl group is solvated by disordered water molecules. In addition, one of the sulfonyl oxygens of **1** approaches closely to the carbonyl oxygen of Gly 216 (3.06 Å). This apparently unfavorable contact may be partially or fully compensated by the close proximity of the sulfur to the same carbonyl oxygen (4.1 Å).

Compounds **2** and **3** are bound with the central Pro in the S_2 pocket and adopt conformations nearly identical to those found in the structures of thrombin complexes with the D-Phe-Pro-Arg-chloromethyl ketone[26] (PPACK), acetyl-D-Phe-Pro-arginine boronic acid[12] (DuP714), and the previously reported structure of the thrombin complex with **2**.[5] Interatomic distances are shown in Figure 5 and suggest that the thrombin complex with **2** is stabilized by three direct hydrogen bonds between the main chain of the peptide inhibitors and enzyme. Compound **3** forms the same three hydrogen bonds with main chain amide and carbonyl groups on thrombin as **2** with interatomic distances of 3.12, 3.12, and 2.86 Å (equivalent to 3.21, 3.15, and 2.72 Å, respectively, in **2**, Figure 5).

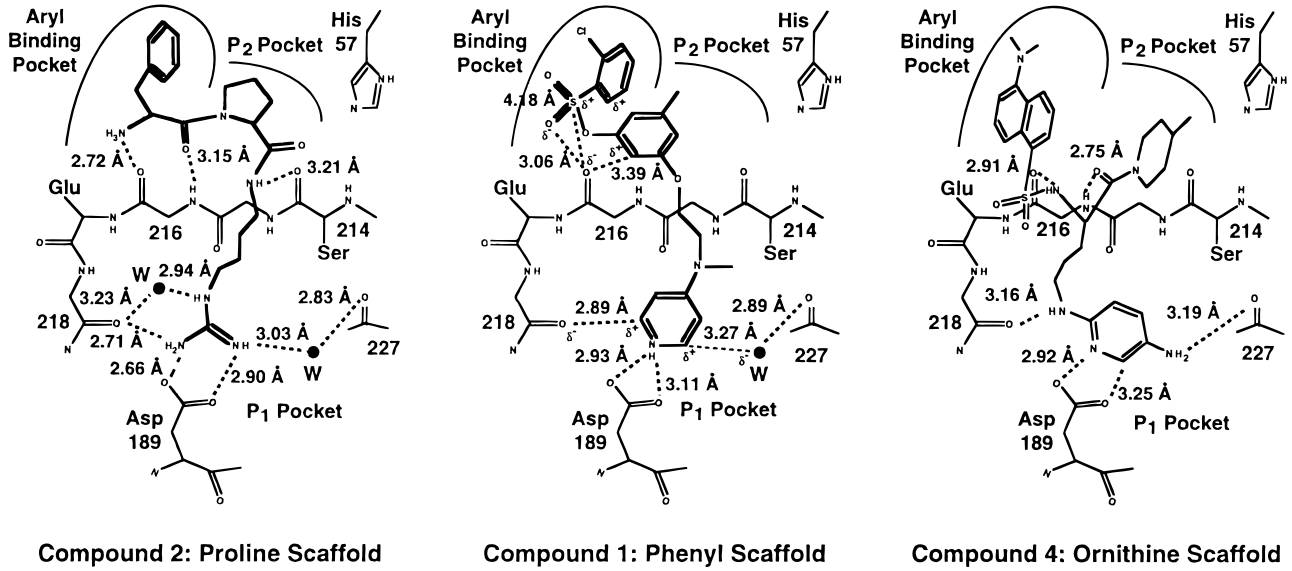

Figure 5. Schematic diagram of the binding modes of peptide compounds **2** and **4** and nonpeptide compound **1**.

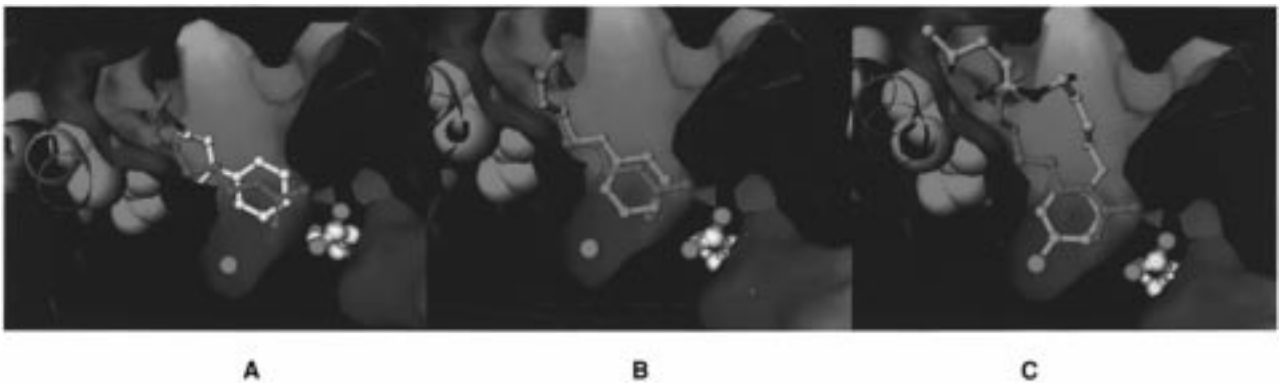

Figure 6. Drawing of the S_1 pocket with the superimposed structures of the thrombin-bound conformations of **2** (magenta) and **1** (white) in panel A, **2** and **3** (red) in panel B, and **2** and **4** (blue) in panel C.

Surprisingly, the central phenyl ring of **1** and Pro of **2** roughly superimpose, but the phenyl ring is displaced by approximately 1 Å so that the C5−C6 bond of **1** partially overlaps with the carbonyl group of the D-Phe residue in **2**. In this binding mode, atoms in the central phenyl ring of **1** appear to overlay exclusively on main chain atoms of peptidyl **2**, with the methyl substituent of **1** projecting into the same space as the side chain Cβ of **2**. The ether linkage in **1**, which connects the phenyl and aminopyridine groups, is displaced by about 1 Å from the position occupied by the amide linkage between Pro and agmatine groups in **2**, thus avoiding an unfavorable contact with the carbonyl group of residue 214. In addition, compound **1** has at least one fewer bonds capable of free rotation (8) compared to **2** (9), and the chloro substituent on **1** may act as a conformational lock to reduce to seven the number of bonds with free rotation.

Compound **4** is bound by the enzyme such that the basic aminopyridine group projects into the S_1 pocket from the position occupied by the P_3 residue of peptide substrates. This mode of interaction allows the central amino acid scaffold to form two hydrogen bonds with Gly 216 on the enzyme (Figure 5) and the carboxy-terminal piperidine to project into the S_2 pocket. The central amino acid scaffold of **4** is displaced by approximately 3 Å from the proline and phenyl scaffolds of **1** and **2** such that there are no equivalent fragments. The methylpiperidine ring is significantly shifted in the S_2 site such that the orientation of the piperidine ring is rotated 90° relative to the orientation of prolyl or orcinol fragments and extends further into the pocket (Figure 4). In this binding mode, the aryl and piperidine substituents straddle the position occupied by the central Pro scaffold in compounds **2** and **3**.

Aminopyridine Interactions with S_1 Pocket. Inhibitors **1** (K_i = 24 nM), **3** (K_i = 4100 nM), and **4** (K_i = 360 nM) utilize *N*,*N*-dialkyl-4-aminopyridine, *N*-alkyl-4-aminopyridine, and *N*-2-alkyl-2,5-diaminopyridine groups, respectively, to substitute for the basic guanidine group in the P_1 position of substrates or inhibitors. The pyridine groups in **1** and **4** substitute for guanidine and maintain equivalent potency while the pyridine substitution in **3** is accompanied by a factor of 20 reduction in potency (ref 27; Table 1). Upon complex formation, the aminopyridine groups of **1**, **3**, and **4** are completely buried in the S_1 pocket and superimpose on the guanidine group of **2** such that the aminopyridine rings occupy the same plane as the guanidine group with the pyridine nitrogens occupying roughly the same position as the guanidine carbon (C25 of **2**; Figure 6). The aminopyridines in **1**, **3**, and **4** are expected to have pK_a values of 9.5, 9.5, and 7.0 based on the pK_a values of *N*-methyl-4-aminopyridine and 2,3-diaminopyridine.[28]

Hydrogen-bonding interactions between the aminopyridine groups of **1**, **3**, and **4** and Asp 189 are shown in Figure 6. While the pyridine nitrogen of **1** has nearly symmetrical interactions with the carboxylate oxygens of Asp 189 (2.93 Å, 3.11 Å), the pyridine nitrogen in **3** is shifted to one side so that the interaction is largely with one carboxylate oxygen (2.70 Å, 3.12 Å) and the pyridine nitrogen in **4** has an entirely asymmetric interaction with Asp 189 (2.92 Å, 3.61 Å). Asp 189 appears to adjust slightly in each complex to optimize the interaction with the pyridine nitrogen.

The edges of the aminopyridine ring systems in **1** and **4** appear in close proximity to electronegative atoms on thrombin or solvent (Figures 5 and 6). In addition, the pyridine ring in **3** remains 3.26 Å from the carbonyl of Gly 218 and 2.89 Å from the buried water molecule. The amino groups in compounds **1** and **3** do not appear to form hydrogen bonds to any enzyme groups or solvent molecules within the thrombin active site. This is in contrast to recently reported structures of thrombin complexes with nonpeptide inhibitors containing an aminopyridine P_1 substituent from which the efficacy of the aminopyridine functionality was attributed in part to the unexpected ability of the amino group to form either a direct or a water-mediated hydrogen bond to the carbonyl of Ser 214.[7] The 2-amino group in **4** does make a hydrogen bond to the carbonyl of Gly 218 (3.16 Å) and the 5-amino group with the carbonyl of Phe 227 (3.19 Å). Of interest is the observation that the 5-amino group in **4** displaces an active site water molecule which is observed in nearly all thrombin inhibitor complexes.[5,7,12,26,29]

Aryl Binding Region. The chlorosulfonyl group of **1** projects into the aryl binding site where it contacts residues Asn 98, Leu 99, Ile 174, and Trp 215 and superimposes nearly exactly on the position occupied by the D-Phe in **2** (Figure 3). The phenyl ring, sulfonate sulfur (S20), and ester oxygen (O8) appear to overlay exactly on the D-Phe phenyl ring, Cβ and Cα atoms. One edge of the chlorophenyl ring of **1** and D-Phe rings of **2** and **3** pack against the face of the Trp 215 side chain and the electron-withdrawing sulfonyl and chloro groups of **1** would be expected to strengthen this electrostatic interaction.[30−32] The 2-chloro substituent projects toward solution and makes no contact with the enzyme. The naphthyl ring of **4** also projects into the aryl binding pocket such that the edge of one ring packs against the face of Trp 215 (Figure 4). However, the orientation and position of the ring are significantly different than the other ring structures. In each of these structures, the aryl substituent appears to be completely removed from solvent but for the one edge.

Hydrophobic Interactions. Although **1** and **2** are similar in terms of molecular weight (neutral species: 432 vs 374), molecular volume (392 vs 372 Å^3), molecular surface area, and molecular surface area buried upon thrombin complex formation (Table 4), **1** has 75 Å^2 more hydrophobic surface than **2**. Upon complex formation, 70 Å^2 more hydrophobic surface area is buried in the thrombin−**1** structure than in the thrombin−**2** structure; 75 Å^2 corresponding to the surface area of approximately three methyl groups.[33] Compound **3** is similar to compound **2** except that slightly more hydrophobic surface area is buried in the thrombin complex with **3**. Compound **4** (539 molecular weight, 534 Å^3 volume) is significantly larger than **1**, **2**, or **3** and buries correspondingly more surface area upon complex formation, although the greatest proportion of the increase is derived from hydrophilic surface area. For each of the compounds the thrombin surface area (hydrophobic and hydrophilic) buried upon complex formation is nearly the same. For these diverse ligands there appears to be no correlation of surface area or buried surface area with ligand affinity.

Table 4. Surface Area Calculations for Thrombin Inhibitor Complexes

	thrombin complex			
surface area	1	2	3	4
ligand	358	348	351	452
hydrophobic	313	238	274	355
hydrophilic	45	110	77	97
ligand buried surface	299	280	284	364
hydrophobic	267	198	235	287
hydrophilic	32	82	49	76
protein buried surface	432	419	414	470
hydrophobic	270	269	261	304
hydrophilic	162	150	153	166
total buried surface	730	699	698	834
hydrophobic	537	467	496	591
hydrophilic	193	232	202	242

Discussion

The active site of thrombin appears to be capable of accommodating a variety of structurally diverse inhibitors. The central phenyl, proline, and ornithine scaffolds of **1**−**4** interact with thrombin in a manner which preserves the projection of substituents into the S_1, S_2, and aryl-binding pockets using apparently low-energy conformations. Surprisingly, the central phenyl ring of **1** substitutes for the main chain atoms of the P_3 amide and P_2 residue of peptidyl **2** rather than the hydrophobic proline ring. In an earlier study, molecular modeling suggested that the tyrosine ring of fibrinogen receptor antagonist **8** might replace the Gly in an Arg-Gly-Asp ligand in a manner very similar to the way in which the phenyl ring of **1** replaces main chain elements in **2**.[1,2] The superior potency of the nonpeptide **1** compared to peptide **2** (Table 1) can be attributed in part to the presence of additional hydrophobic interactions and reduced degrees of conformational flexibility in the nonpeptide. However, the potency of **1** remains surprising in view of the absence of direct hydrogen-bonding interactions between **1** and residues Ser 214 and Gly 216 of thrombin which typically interact with the P_1 and P_3 main chain atoms of substrates or peptide-based inhibitors such as **2**.

Upon complex formation between thrombin and **1**, four or five hydrogen-bond donor or acceptor sites on the enzyme and two hydrogen-bond acceptor sites on **1** become buried. The crystallographic data provide no evidence that ordered solvent molecules are buried or otherwise partially solvate these sites. Instead, these thrombin hydrogen-bonding groups appear to be juxtaposed with inhibitor groups which are expected to carry complementary partial charges. The edges of the central phenyl and aminopyridine rings and the sulfonyl sulfur of **1**, anticipated to carry partial positive charge, are in close contact with enzyme carbonyl groups, which are expected to carry partial negative charge (Figures

3 and 6). The ability of these weak electrostatic interactions to contribute to intermolecular interactions has been studied in a number of theoretical and crystallographic studies[30,34−44] and has been noted previously for the thrombin interaction with aminopyridines.[7]

Previously, aminopyridine-containing thrombin inhibitors have been observed to form a direct hydrogen bond between the 4-amino group and the carbonyl group of Ser 214 on the enzyme.[7] In the present work, two additional modes of aminopyridine interaction are observed and significant flexibility is observed in the positioning of the pyridine ring systems in the S_1 pocket and in the mode of interaction of the pyridine functionality with Asp 189. This may result from the ability of these ring systems to participate in weak electrostatic interactions (Figure 6). In the thrombin complex with **3**, the 4-amino group does not form a hydrogen bond to either enzyme or solvent, while in the complex with **4** both 2-amino and 5-amino groups appear to find hydrogen-bonding partners. The aminopyridine group in **4** (K_i = 360 nM), which retains the ability to form two hydrogen bonds with the S_1 pocket, substitutes for a guanidine without loss in activity (Table 1). However, on the basis of the potency of compound **1** (K_i = 24 nM) and the inability of **1** to donate a hydrogen bond to the enzyme, it is not clear that participation of pyridine amino groups in hydrogen bonding contributes significantly to the free energy of binding to thrombin. The reduced potency of compound **3** (K_i = 4100 nM) compared to **2** (K_i = 180 nM) suggests that the efficacy of aminopyridine functional groups as guanidine replacements may depend in large part on the effectiveness of the scaffold in presenting the groups appropriately.

The superior binding potency of nonpeptides, such as **1**, compared with peptide ligands, such as **2**, may derive in large part from the greater ease with which the nonpeptides can be removed from solvent water. During the binding process, the protein and the ligand must each be desolvated in an energetically costly process before they can combine in an energetically productive process in which intermolecular interactions are formed.[45] Compounds **1** and **2** have the same sized surfaces and volumes and interact with similarly sized hydrophobic and hydrophilic surfaces on thrombin, so desolvation of the thrombin active site in each complex is nearly identical. However, the aryl ether linkage which connects the central phenyl and aminopyridine groups in **1** is 10^5-fold more easily extracted from water into the vapor phase than the amide linkage which connects the central prolyl and guanidino groups in **2**.[45] The neutral pyridine group in **1** is 10^5-fold more easily removed from solvent water than the neutral guanidine group in **2**.[45] Similarly, on the basis of water−octanol partition coefficients for phenyl benzenesulfonate and *N*-phenylbenzamide,[46] the ester linkage connecting the central phenyl and chlorophenyl rings is expected to be more easily extracted from water than the amide linkage connecting D-Phe and Pro residues in **2**.

Conclusions

The thrombin substrate binding site is degenerate in its ability to accommodate a variety of structurally diverse inhibitors which project equivalent substituents into the same binding subsites from differert scaffolds. Our data provide additional detail and insight concerning how one phenyl scaffold maps onto the peptide residue that it replaces and how substituents project off the scaffold into binding subsites on the drug target. The affinity of nonpeptide **1** for thrombin appears to be a consequence of excellent hydrophobic interactions between **1** and thrombin and the ease of desolvation of **1**; the juxtaposition of complementary partial charges on **1** and thrombin may also contribute to affinity. The aminopyridine groups on **1**, **3**, and **4** appear to be versatile guanidine substitutes which can interact in a number of ways with the S_1 pocket of tryptic proteases, have reduced pK_a values, and are readily extracted from solvent.

In the future, when the structure of a drug target is determined complexed with a natural peptide ligand or peptide lead it will be possible to compare the bound conformation of the peptide to the thrombin bound conformations of **2** and **1** to know whether the phenyl group in **1** will be a suitable scaffold for the new target binding site. By establishing a structural database for a series of corresponding target−nonpeptide and target−peptide complexes, it should be possible to rapidly identify a suitable nonpeptide scaffold for new drug targets for which structural data with peptide leads exists. Database approaches such as this have shown tremendous utility in protein design and protein structure prediction.[47,48]

References

(1) Hartman, G. D.; Egbertson, M. S.; Halczenko, W.; Laswell, W. L.; Duggan, M. E.; Smith, R. S.; Naylor, A. M.; Manno, P. D.; Lynch, R. L.; Zhang, G.; Chang, C. T.-C.; Gould, R. J.Non-Peptide Fibrinogen Receptor Antagonists. 1. Discovery and Design of Exosite Inhibitors. *J. Med. Chem.* **1992**, *35*, 4640−4642.

(2) Egbertson, M. S.; Chang, C. T.-C.; Duggan, M. E.; Gould, R. J.; Halczenko, W.; Hartman, G. D.; Laswell, W. L.; Lynch, J. J. Jr.; Lynch, R. L.; Manno, P. D.; Naylor, A. M.; Prugh, J. D.; Ramjit, D. R.; Sitko, G. R.; Smithe, R. S.; Turchi, L. M.; Zhang, G. Non-Peptide Fibrinogen Receptor Antagonists. 2. Optimization of a Tyrosine Template as a Mimic for Arg-Gly-Asp. *J. Med. Chem.* **1994**, *37*, 2537−2551.

(3) Qian, Y.; Vogt, A.; Sebti, S. M.; Hamilton, A. D. Design and Synthesis of Non- Peptide Ras CAAX Mimetics as Potent Farnesyltransferase Inhibitors. *J. Med Chem.* **1996**, *39*, 217−223.

(4) Qian Y.; Blaskovich, M. A.; Seong, C. M.; Vogt, A.; Hamilton, A. D.; Sebti, S. M. Peptidomimetic Inhibitors of P21Ras Farnesyltransferase: Hydrophobic Functionalization Leads to Disruption of P21Ras Membrane Association in Whole Cells. *Bioog. Med. Chem. Lett.* **1994**, *4*, 2579−2584.

(5) Wiley: M. R.; Chirgadze, N. Y.; Clawson, D. K.; Craft, T. J.; Gifford-Moore, D. S.; Jones, N. D.; Olkowski, J. L.; Schacht, A. L.; Weir, L. C.; Smith, G. F. Serine Protease Selectivity of the Thrombin Inhibitor D-Phe-Pro-Agmatine and its Homologs. *Bioorg. Med. Chem. Lett.* **1995**, *5*, 2835−2840.

(6) von der Saal, W.; Heck, R.; Leinert, H.; Poll, T.; Stegmeier, K.; Michel, H. New 4-Aminopyridines, Process for Preparing the Same and Medicaments Containing the Same. WO 94/20467 **1994**.

(7) Engh, R. A.; Brandsetter, H.; Sucher, G.; Eichinger, A.; Baumann, U.; Bode, W.; Huber, R.; Poll, T.; Rudolph, R.; von der Saal, W. Enzyme flexibility, solvent and 'weak' interactions characterize thrombin-ligand interactions: implications for drug design. *Structure* **1996**, *4*, 1353−1362.

(8) Tucker, T. J.; Lumma, W. C.; Mulichak, A. M.; Chen, Z.; Naylor-Olsen, A. M.; Lewis, S. D.; Lucas, R.; Freidinger, R. M.; Kuo, L. C. Design of Highly Potent Noncovalent Thrombin Inhibitors That Utilize a Novel Lipophilic Binding Pocket in the Thrombin Active Site. *J. Med. Chem.* **1997**, *40*, 830−832.

(9) Tucker, T. J.; Lumma, W. C.; Lewis, S. D.; Gardell, S. J.; Lucas, B. J.; Baskin, E. P.; Woltmann, R.; Lynch, J. J.; Lyle, E. A.; Appleby, S. D.; Chen, I.-W.; Dancheck, K. B.; Vacca, J. P. Potent Noncovalent Thrombin Inhibitors That Utilize the Unique Amino Acid D-Dicyclohexylalanine in the P3 Position. Implications on Oral Bioavailability and Antithrombotic Efficacy. *J. Med. Chem.* **1997**, *40*, 1565−1569.

(10) Feng, D.-M.; Gardell, S. J.; Lewis, S. D.; Bock, M. G.; Chen, Z.; Freidinger, R. M.; Naylor-Olsen, A. M.; Ramjit, H. G.; Woltmann, R.; Baskin, E. P.; Lynch, J. J.; Lucas, R.; Shafer, J. A.; Dancheck, K. B.; Chen, I.-W.; Mao, S.-S.; Krueger, J. A.; Hare, T. R.; Mulichak, A. M.; Vacca, J. P. Discovery of a Novel, Selective, and Orally Bioavailable Class of Thrombin Inhibitors Incorporation Aminopyridyl Moieties at the P1 Position. *J. Med. Chem.* **1997**, *40*, 3726−3733.

(11) Schechter, I.; Berger, A. On the Size of the Active site in Proteases. I. Papain. *Biochem. Biophys. Res. Commun.* **1967**, *27*, 157.

(12) Webber, P. C.; Lee, S.-L.; Lewandowski, F. A.; Schadt, M. C.; Chang, C.-H., Kettner, C. A. Kinetic and Crystallographic Studies of Thrombin with Ac-(D)Phe-Pro-boroArg-OH and Its Lysine, Amidine, Homolysine and Ornithine Analogs. *Biochemistry* **1995**, *34*, 3750−3757.

(13) Skrzypczak-Jankun, E.; Carperos, V.; Ravichandran, K. G.; Tulinsky, A.; Westbrook, M.; Maraganore, J. M. Structure of the Hirugen and Hirulog 1 Complexes of α-Thrombin. *J. Mol. Biol.* **1991**, *221*, 1379−1393.

(14) Bajusz, S.; Szell, E.; Barabas, E.; Bagdy, D.; Zsuzsanna, M. Novel Anticoagulant Agmatine Derivatives and Process for the Preparation Thereof. U.S. Patent 4,346,078 August 24, 1982.

(15) Graybill, T. L.; Agrafiotis, D. K.; Bone, R.; Illig, C. R.; Jaeger, E. P.; Locke, K. T.; Lu, T.; Salvino, J. M.; Soll, R. M.; Spurlino, J. C.; Subasinghe, N.; Tomczuk, B. E.; Salemme, F. R. Enhancing the Drug Discovery Process by Integration of High-Throughput Chemistry and Structure-Based Drug Design. In *Molecular Diversity and Combinatorial Chemistry: Libraries for Drug Discovery*; *ACS* Monograph; American Chemical Society: Washington, DC, 1996; pp 16−27.

(16) Brunger, A. T.; Kuriyan, J.; Karplus, M. Crystallographic R−Factor Refinement by Molecular Dynamics. *Science* **1987**, *235*, 458−460.

(17) Sack, J. S. CHAIN-a Crystallographic Modeling Program. *J. Mol. Graphics* **1988**, *249*, 224−225.

(18) Connolly, M. L. Analytical Molecular Surface Calculation. *J. Appl. Crystallogr.* **1983**, *16*, 548−558.

(19) Connolly, M. L. Solvent-Accessible Surfaces of Proteins and Nucleic Acids. *Science* **1983**, *221*, 709−713.

(20) Bernstein, F. C.; Koetzle, T. F.; Meyer, E. F., Jr.; Brice, M. D.; Rodgers, J. R.; Kennard, O.; Shimanouchi, T.; Tasumi, M. The Protein Databank: A Computer Based Archival File for Macro-Molecular Structures. *J. Mol. Biol.* **1977**, *112*, 535−542.

(21) Prince, P.; Fronczek, F. R.; Gandour, R. D. 2,7-Naphthalenediyl Bis(*p*- toluenesulfonate) *Acta Crystallogr.* **1991**, *C47*, 220−222.

(22) White, D. N. J.; McPhail, A. T.; Sim, G. A. X-Ray Study of the Molecular Structure of 4-Demethylhasubanonine *p*-Bromobenzenesulphonate. *J. Chem. Soc., Perkin Trans. 2* **1972**, 1280−1283.

(23) Bindal, R. D.; Golab, J. T.; Katzenellenbogen, J. A. Ab Initio Calculations on *N*-Methylmethanesulfonamide and Methyl Methanesulfonate for the Development of Force Field Torsional Parameters and Their Use in the Conformational Analysis of Some Novel Estrogens. *J. Am. Chem. Soc.* **1990**, *112*, 7861−7868.

(24) Cevasco, G.; Penco, S.; Thea, S.; Busetti, V. J. Crystal structure of the cyclic tetramer from 3,5-dichloro-4-hydroxybenzenesulfonylchloride. *Chem. Res.* **1993**, *102*, 779−780.

(25) Nohara, T.; Kinjo, J.; Furusawa, J.; Sakai, Y.; Inoue, M.; Shirataki, Y.; Ishibashi, Y.; Yokoe, I.; Komatsu, M. But-2-enolides from Pueraria Lobata and Revised Structures of Puerosides A, B, and Sophoroside A. *Phytochemistry* **1993**, *33*, 1207−1210.

(26) Bode, W.; Mayr, I.; Baumann, U.; Huber, R.; Stone, S. R.; Hofsteenge, J. The refined 1.9 Å crystal structure of human α-thrombin: interaction with D-Phe-Pro-Arg chloromethylketone and significance of the Tyr-Pro-Pro-Trp insertion segment. *EMBO J.* **1989**, *8*, 3467−3475.

(27) Lu, T.; Illig, C. R.; Tomczuk, B. E.; Soll, R. M.; Subasinghe, N. L.; Bone, R. F. Guanidino Protease Inhibitors. WO 97/11693, 1997.

(28) Fasman, G. D. Ionization Constants of Acids and Bases. *Handbook of Biochemistry and Molecular Biology* 3rd ed.; CRC Press, Inc.: Boca Raton, FL, 1976.

(29) Stubbs, M. T.; Oschkinat, H.; Mayr, I.; Huber, R.; Angliker, H.; Stone, S. R.; Bode, W. The Interaction of Thrombin with Fibrinogen: a Structural Basis for its Specificity. *Eur. J. Biochem.* **1992**, *206*, 187−195.

(30) Burley, S. K.; Petsko, G. A. Aromatic−Aromatic Interaction: A Mechanism of Protein Structure Stabilization. *Science* **1985**, *229*, 23−28.

(31) Cox, E. G.; Cruikshank, D. W. J.; Smith, J. A. The Crystal Structure of Benzene at 30 °C. *Proc. R. Soc. London* **1958**, *A247*, 1.

(32) Janda, K. C.; Hemminger, J. C.; Winn, J. S.; Novick, S. E.; Harris, S. J.; Klemperer, W. J. Benzene Dimer. Polar Molecule. *J. Chem. Phys.* **1975**, *63*, 1419.

(33) Richards, F. M. Areas, volumes, packing and protein structure. *Annu. Rev. Biophys. Bioeng.* **1977**, *6*, 151−176.

(34) Desiraju, G. The C−H···O Hydrogen Bond: Structural Implications and Supromolecular Design. *Acc. Chem. Res.* **1996**, *29*, 441−449.

(35) Glusker, J. P. Intermolecular Interactions Around Functional Groups in Crystals: Data for Modeling the Binding of Drugs to Biological Macromolecules. *Acta Crystallogr.* **1995**, *D51*, 418−427.

(36) Taylor, R.; Kennard, O. Crystallographic Evidence for the Existence of C−H···O, C−H···N, and C−H···Cl Hydrogen Bonds. *J. Am. Chem. Soc.* **1982**, *104*, 5063−5070.

(37) Derewenda, Z. S.; Lee, L.; Derewenda, U. The Occurrence of C−H···O Hydrogen Bonds in Proteins. *J. Mol. Biol.* **1995**, *252*, 248−262.

(38) Derewenda, Z. S.; Derewenda, U.; Kobos, P. M. (His)C^{ϵ}-H···O=C< Hydrogen Bond in the Active Sites of Serine Hydrolases. *J. Mol. Biol.* **1994**, *241*, 83−93.

(39) Steiner, T.; Saenger, W. Role of C−H···O Hydrogen Bonds in the Coordination of Water Molecules. Analysis of Neutron Diffraction Data. *J. Am. Chem. Soc.* **1993**, *115*, 4540−4547.

(40) Seiler, P.; Dunitz, J. D. An Eclipsed C(sp^3)-CH_3 Bond in a Crystalline Hydrated Tricyclic Orthoamide: Evidence for C−H···O Hydrogen Bonds. *Helv. Chim. Acta* **1989**, *72*, 1125−1135.

(41) Steiner, T. Water Molecules Which Apparently Accept No Hydrogen Bonds are Systematically Involved in C−H···O Interactions. *Acta Crystallogr.* **1995**, *D51*, 93−97.

(42) Pascard, C. Small-Molecule Crystal Structures as a Structural Basis for Drug Design. *Acta Crystallogr.* **1995**, *D51*, 407−417.

(43) Burley, S. K.; Petsko, G. A. Dimerization Energetics of Benzene and Aromatic Amino Acid Side Chains. *J. Am. Chem. Soc.* **1986**, *108*, 7995−8001.

(44) Burley, S. K.; Petsko, G. A. Weakly Polar Interactions in Proteins. *Adv. Protein Chem.* **1988**, *39*, 125−189.

(45) Wolfenden, R. Waterlogged Molecules. *Science* **1983**, *222*, 1087−1093.

(46) Hansch, C., Leo, A. Substituent Constants for Correlational Analysis in Chemistry and Biology, John Wiley and Sons: New York, 1979.

(47) Finzel, B. C.; Kimatian, S.; Ohlendorf, D. H.; Wendoloski, J. J.; Levitt, M.; Salemme, F. R. Molecular Modeling with Substructure Libraries Derived from Known Protein Structures. In *Crystallographic and Modeling Methods in Molecular Design*; Ealick, S., Bugg, C., Eds.; Springer-Verlag: New York, 1990; pp 175−189.

(48) Horlick, R. A.; George, H. J.; Cooke, G. M.; Tritch, R. J.; Newton, R. C.; Dwivedi, A.; Lischwe, M.; Salemme, F. R.; Weber, P. C.; Horuk, R. Permuteins of Interleukin 1β−a Simplified Approach for the Construction of Permuted Proteins Having New Termini. *Protein Eng.* **1992**, *5*, 427−431.

(49) Okamoto, S.; Hijikata-Okunomiya, A. Synthetic Selective Inhibitors of Thrombin. *Methods Enzymol.* **1993**, *222*, 328−340.

JM970796L